

Measuring Parton Energy Loss at RHIC compared to LHC

M. J. Tannenbaum[‡], PHENIX Collaboration

Physics Department, Brookhaven National Laboratory, Upton, NY 11973-5000, USA

E-mail: mjt@bnl.gov

Abstract. The method of measuring $\hat{x}_h = \hat{p}_{Ta}/\hat{p}_{Tt}$, the ratio of the away-parton transverse momentum, \hat{p}_{Ta} , to the trigger-parton transverse momentum, \hat{p}_{Tt} , using two-particle correlations at RHIC, will be reviewed. This measurement is simply related to the two new variables introduced at LHC for the di-jet fractional transverse momentum imbalance: ATLAS $A_J = (\hat{p}_{Tt} - \hat{p}_{Ta})/(\hat{p}_{Tt} + \hat{p}_{Ta}) = (1 - \hat{x}_h)/(1 + \hat{x}_h)$; and CMS $\langle(\hat{p}_{Tt} - \hat{p}_{Ta})/\hat{p}_{Tt}\rangle = \langle 1 - \hat{x}_h \rangle$. Results from two-particle correlations at RHIC for \hat{x}_h in p-p and A+A collisions will be reviewed and new results will be presented and compared to LHC results. The importance of comparing any effect in A+A collisions to the same effect in p-p collisions will be illustrated and emphasized.

1. Introduction

In 1998, at the QCD workshop in Paris, Rolf Baier asked me whether jets could be measured in Au+Au collisions because he had a prediction of a QCD medium-effect (energy loss via soft gluon radiation induced by multiple scattering [1] on color-charged partons traversing a hot-dense-medium composed of screened color-charges [2]). I told him [3] that there was a general consensus [4] that for Au+Au central collisions at $\sqrt{s_{NN}} = 200$ GeV, leading particles are the only way to study jets, because in one unit of the nominal jet-finding cone, $\Delta r = \sqrt{(\Delta\eta)^2 + (\Delta\phi)^2}$, there is an estimated $\pi\Delta r^2 \times \frac{1}{2\pi} \frac{dE_T}{d\eta} \sim 375$ GeV of energy (!!) The good news was that hard-scattering in p-p collisions was originally observed by the method of leading particles and that these techniques could be used to study hard-scattering and jets in Au+Au collisions [5].

2. Hard scattering via single particle inclusive and two-particle correlation measurements

Single particle inclusive and two-particle correlation measurements of hard-scattering have provided a wealth of discoveries at RHIC. Due to the steeply falling power-law invariant transverse momentum spectrum of the scattered parton, \hat{p}_{Tt}^{-n} , the inclusive single particle (e.g. π^0) p_{Tt} spectrum from jet fragmentation is dominated by fragments

[‡] Supported by the U.S. Department of Energy, Contract No. DE-AC02-98CH1-886.

with large z_{trig} , where $z_{\text{trig}} = p_{T_t}/\hat{p}_{T_t}$ is the fragmentation variable, and exponential fragmentation $D_q^{\pi^0}(z) \sim e^{-bz}$ is assumed. This gives rise to several effects which allow precision measurements of hard scattering to be made using single inclusive particle spectra and two particle correlations [6, 7].

The prevailing opinion from the 1970's until quite recently was that although the inclusive single particle (e.g. π^0) spectrum from jet fragmentation is dominated by trigger fragments with large $\langle z_{\text{trig}} \rangle \sim 0.6 - 0.8$, the away-jets should be unbiased and would measure the fragmentation function, once the correction is made for $\langle z_{\text{trig}} \rangle$ and the fact that the jets don't exactly balance p_T due to the k_T smearing effect [8]. Two-particle correlations with trigger p_{T_t} , are analyzed in terms of the two variables: $p_{\text{out}} = p_T \sin(\Delta\phi)$, the out-of-plane transverse momentum of an associated track with p_T ; and x_E , where:

$$x_E = \frac{-\vec{p}_T \cdot \vec{p}_{Tt}}{|p_{Tt}|^2} = \frac{-p_T \cos(\Delta\phi)}{p_{Tt}} \simeq \frac{z}{z_{\text{trig}}} \quad \text{JET} \leftarrow \begin{array}{c} \text{Trigger } p_{T_t} \\ \uparrow \\ j_{T_t} \end{array} \quad \begin{array}{c} p_T \\ \uparrow \\ j_T \end{array} \rightarrow \text{JET} \quad \begin{array}{c} p_{\text{out}} \\ \uparrow \\ k_T \end{array}$$

$z_{\text{trig}} \simeq p_{T_t}/p_{T_{\text{jet}}}$ is the fragmentation variable of the trigger jet, and z is the fragmentation variable of the away jet.

However, in 2006, it was found by explicit calculation that this is not true [9, 6, 7]. The shape of the p_{T_a} spectrum of fragments (from the away-side parton with \hat{p}_{T_a}), given a trigger particle with p_{T_t} (from a trigger-side parton with \hat{p}_{T_t}), is not sensitive to the shape of the fragmentation function (b), but measures the ratio of \hat{p}_{T_a} of the away-parton to \hat{p}_{T_t} of the trigger-parton and depends only on the same power n as the invariant single particle spectrum:

$$\left. \frac{dP_{p_{T_a}}}{dx_E} \right|_{p_{T_t}} \approx \langle m \rangle (n-1) \frac{1}{\hat{x}_h} \frac{1}{(1 + \frac{x_E}{\hat{x}_h})^n} \quad . \quad (1)$$

This equation gives a simple relationship between the ratio, $x_E \approx p_{T_a}/p_{T_t} \equiv z_T$, of the transverse momenta of the away-side particle to the trigger particle, and the ratio of the transverse momenta of the away-jet to the trigger-jet, $\hat{x}_h = \hat{p}_{T_a}/\hat{p}_{T_t}$. The only dependence on the fragmentation function is in the mean multiplicity $\langle m \rangle$ of jet fragments. This functional form was shown previously [9, 10] (and with the present data, see below) to describe the π^0 triggered x_E distribution in p-p collisions and is based only on the following simplifying assumptions: the hadron fragment is assumed to be collinear with the parton direction; the underlying fragmentation functions ($D(z)$) are assumed to be exponential; and for a given p_{T_t} , \hat{x}_h is taken to be constant as a function of x_E over the range of interest. The key issue with Eq. 1 is that it is independent of the slope of an exponential fragmentation function, and only depends on the detected mean multiplicity $\langle m \rangle$ of the jet, the power, n , of the inclusive p_{T_t} spectrum and the ratio of the away jet to the trigger jet transverse momenta, \hat{x}_h .

3. Fits to PHENIX π^0 -h correlations

The two-particle correlation distributions from π^0 triggers in four intervals of p_{T_t} , 4-5, 5-7, 7-9 and 9-12 GeV/c, with charged hadrons in a fixed range of associated transverse

momenta, $p_{T_a} \approx 0.7, 1.3, 2.3, 3.5, 5.8$ GeV/c were recently published by PHENIX [11] in terms of the ratio of A+A to p-p collisions, $I_{AA}(p_{T_a})|_{p_{T_t}} = \frac{dP^{AA}/dp_{T_a}}{dP^{pp}/dp_{T_a}}|_{p_{T_t}}$ (see Fig. 1).

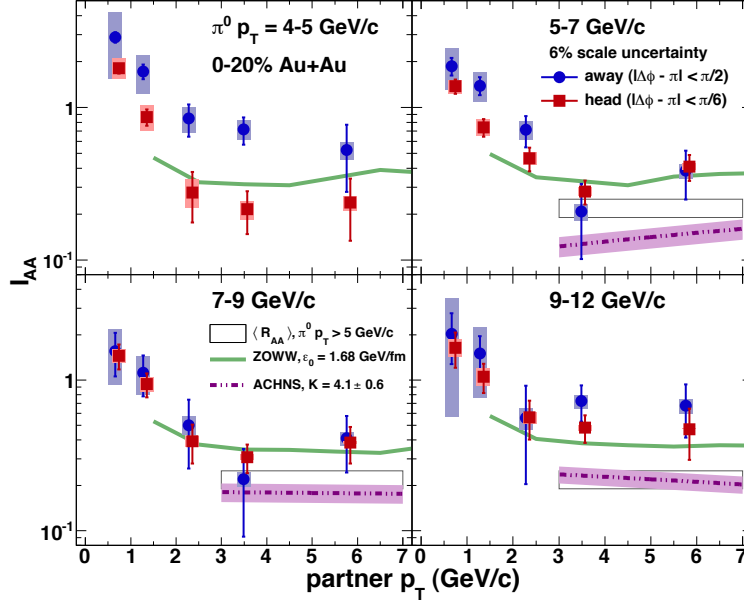


Figure 1. Away-side I_{AA} [11] for a narrow “head” $|\Delta\phi - \pi| < \pi/6$ selection (solid squares) and the entire away-side, $|\Delta\phi - \pi| < \pi/2$ (solid circles) as a function of partner momentum p_{T_a} for various trigger momenta p_{T_t} . Only the head region was used for the present analysis.

We now analyze these distributions separately for p-p and Au+Au collisions, with the statistical error and the larger of the \pm systematic errors of the data points added in quadrature. The p-p and Au+Au distributions in $z_T = p_{T_a}/p_{T_t}$ were fit to the formula [9]:

$$\left. \frac{dP_\pi}{dz_T} \right|_{p_{T_t}} = N(n-1) \frac{1}{\hat{x}_h} \frac{1}{(1 + \frac{z_T}{\hat{x}_h})^n}, \quad (2)$$

with a fixed value of $n = 8.10 (\pm 0.05)$ as previously determined [12], where n is the power-law of the inclusive π^0 spectrum and is observed to be the same in p-p and Au+Au collisions in the p_{T_t} range of interest. The fitted value for N is the integral of the z_T distribution which equals $\langle m \rangle$, the mean multiplicity of the away jet in the PHENIX detector acceptance, and $\hat{x}_h \equiv \hat{p}_{T_a}/\hat{p}_{T_t}$ is the ratio of the away jet to the trigger jet transverse momenta.

Fits were performed for the p-p spectra; and also for the Au+Au spectra at two centralities: 0-20% and 20-40% upper-percentiles. The parameters of the p-p distribution, \hat{x}_h^{pp} and N_{pp} , are determined by fits of Eq. 2 to the p-p data for the four intervals of p_{T_t} ; and the parameters \hat{x}_h^{AA} and N_{AA} are determined from the fits to the Au+Au distributions. The fits were performed only for the narrower “head” region, $|\Delta\phi - \pi| < \pi/6$. It should be noted that in Fig. 1, there is no difference in the results (I_{AA}) for the full away side and the head region, for $p_{T_t} \geq 7$ GeV/c, because the non-jet

background becomes sufficiently small so that the “shoulder” [13], now known to be due to a v_3 background modulation [14] for which no correction has been applied in this data, contributes negligibly to the away-side yield.

4. Results of the fits

Examples of the fits for $7 < p_{T_i} < 9$ GeV/c for p-p collisions and Au+Au 0–20% and 20–60% are shown in Figs. 2a and b, respectively. The results for the fitted parameters

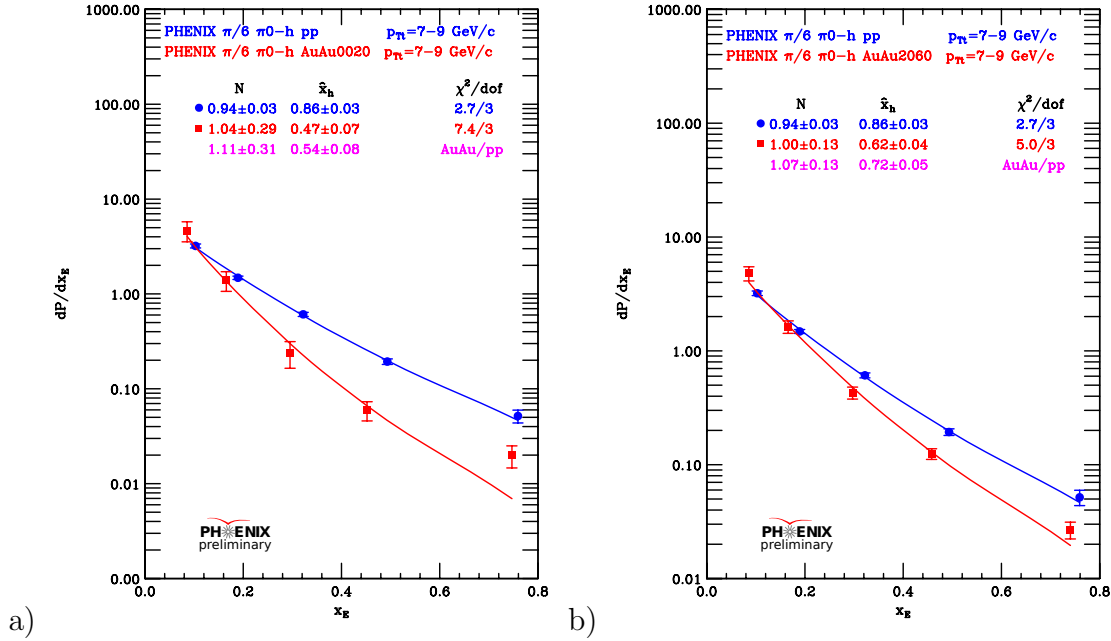


Figure 2. p-p (blue circles) and AuAu (red squares) $z_T = p_{T_a} / \langle p_{T_i} \rangle$ distributions for $p_{T_i} = 7 - 9$ GeV/c ($\langle p_{T_i} \rangle = 7.71$ GeV/c), together with fits to Eq. 2 p-p (solid blue line), AuAu (solid red line) with parameters indicated: a) 00-20% centrality, b) 20–60% centrality. The ratios of the fitted parameters for AuAu/pp are also given.

are shown on the figures. In general the values of \hat{x}_h^{pp} do not equal 1 but range between $0.8 < \hat{x}_h^{pp} < 1.0$ due to k_T smearing and the range of z_T covered. For the fixed range of associated p_{T_a} 0.7 – 5.8 GeV/c, the lowest $p_{T_i} = 4 - 5$ GeV/c trigger provides the most balanced same and away side jets, with $\hat{x}_h \approx 1.0$, while as p_{T_i} increases up to 9–12 GeV/c, for the fixed range of p_{T_a} , the jets become unbalanced towards the trigger side in p-p collisions due to k_T smearing. Thus, in the present data, the p_{T_i} and z_T ranges are identical for the p-p and Au+Au comparison. Furthermore, in order to take account of the imbalance ($\hat{x}_h^{pp} < 1$) observed in the p-p data, the ratio $\hat{x}_h^{AA} / \hat{x}_h^{pp}$ is taken as the measure of the energy of the away jet relative to the trigger jet in A+A compared to p-p collisions.

It is important to note that the away jet energy fraction in AuAu relative to p-p, $\hat{x}_h^{AA} / \hat{x}_h^{pp} = 0.47/0.86 = 0.54 \pm 0.08$ in Fig. 2a, is significantly less than 1, indicating energy loss of the away jet in the medium. Also since the away-jet may suffer different

energy losses for a given trigger jet \hat{p}_{T_t} due to variations in the path-length through the medium, \hat{x}_h^{AA} should be understood as $\langle \hat{x}_h^{AA} \rangle$.

5. LHC Results

In very exciting first results from the LHC heavy ion program, ATLAS [15] observed dijet events in Pb+Pb central collisions at $\sqrt{s_{NN}} = 2.76$ TeV with a large energy asymmetry which they characterized by a new quantity $A_J = (1 - \hat{x}_h^{AA}) / (1 + \hat{x}_h^{AA})$. Shortly thereafter, CMS [16] presented a plot of $\langle 1 - p_{t,2}/p_{t,1} \rangle = 1 - \langle \hat{x}_h^{AA} \rangle$, the fractional jet imbalance as a function of E_{T1} up to 200–220 GeV with a cut $E_{T2} \geq 50$ GeV (Fig. 3). If there were no cuts on the p-p jets used in this measurement, then this variable should be identical to the one we call $1 - \hat{x}_h^{AA}/\hat{x}_h^{pp}$, the away-parton fractional energy loss (or imbalance) in A+A relative to p-p. However, due to the cut used in the CMS data, the sample of di-jets

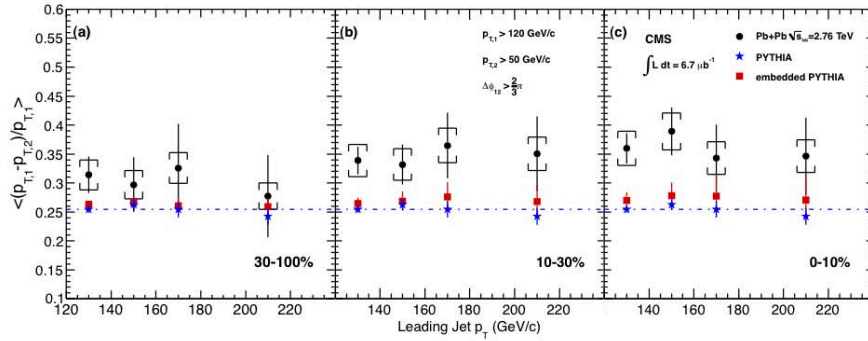


Figure 3. CMS [16] plot of $\langle 1 - p_{t,2}/p_{t,1} \rangle$, the fractional jet imbalance, as a function of $p_{t,1}$ for 3 centralities in p-p and Pb+Pb collisions.

in p-p used to compare with A+A suffers from a large imbalance of 0.25, independent of E_{T1} (Fig. 3). We correct this by calculating \hat{x}_h^{AA} and \hat{x}_h^{pp} for CMS from their given values of $1 - \hat{x}_h^{AA}$ and $1 - \hat{x}_h^{pp}$ and then correcting to $1 - \hat{x}_h^{AA}/\hat{x}_h^{pp}$. For instance, in Fig. 3c for $E_{T1} = 130$ GeV, $\langle 1 - \hat{x}_h^{pp} \rangle = 0.255$ (i.e. $\langle \hat{x}_h^{pp} \rangle = 0.745$), while $\langle 1 - \hat{x}_h^{AA} \rangle = 0.36$ (i.e. $\langle \hat{x}_h^{AA} \rangle = 0.64$), so that $1 - \langle \hat{x}_h^{AA} \rangle / \langle \hat{x}_h^{pp} \rangle = 1 - (0.64/0.745) = 0.141$.

The corrected points are shown together with the PHENIX data for $1 - \hat{x}_h^{AA}/\hat{x}_h^{pp}$, which we denote for simplicity $\langle 1 - \hat{x}_h \rangle$, the observed fractional jet imbalance in A+A relative to p-p (Fig. 4). Of course the CMS result is directly measured with jets, while the PHENIX value is deduced from the fragments of the dijets using a few simple assumptions, as noted above. The PHENIX data are plotted at the presumed mean trigger parton transverse momentum $\langle \hat{p}_{T_t} \rangle = p_{T_t} / \langle z_{\text{trig}} \rangle$, where the average fragmentation fraction of the trigger particle, $\langle z_{\text{trig}} \rangle \approx 0.7$, was derived in Ref. [9]. There is a clear difference in fractional jet imbalance in going from RHIC to LHC in central collisions—the jet-imbalance or fractional energy loss is much smaller at LHC. This is different from the first impression [15]. Also at RHIC, there is less fractional energy loss or jet imbalance in less central collisions.

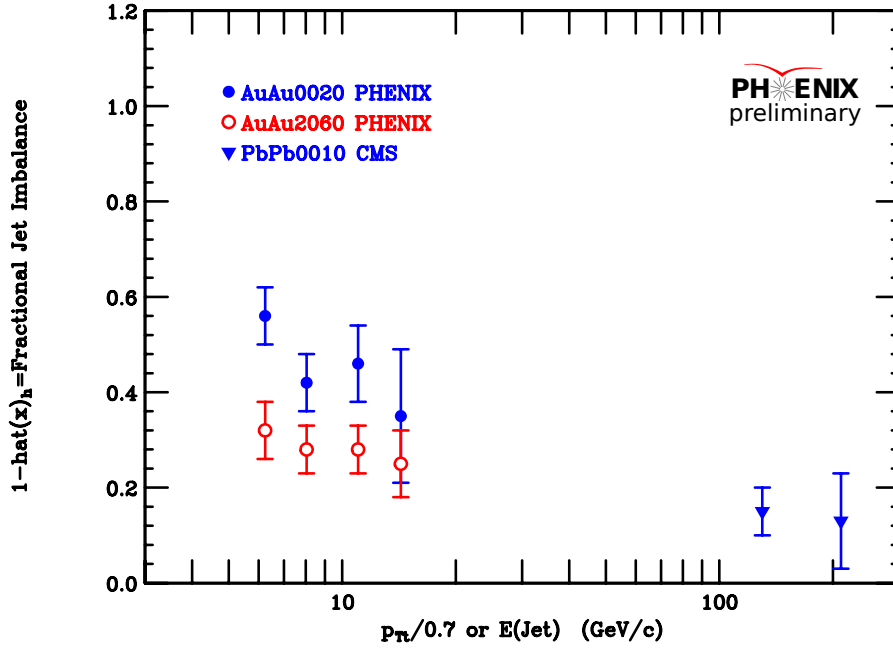


Figure 4. Away-jet fractional imbalance or energy loss in A+A relative to p-p, $1 - \hat{x}_h$, as a function of $p_{T_t}/0.7$ for PHENIX and $E(\text{Jet})$ for CMS, with centralities indicated.

The large difference in fractional jet imbalance between RHIC and LHC c.m. energies could be due to the difference in jet \hat{p}_{T_t} between RHIC (~ 20 GeV/c) and LHC (~ 200 GeV/c), the difference in n for the different \sqrt{s} , or to a difference in the properties of the medium. Future measurements will need to sort out these issues by extending both the RHIC and LHC measurements to overlapping regions of p_T .

References

- [1] R. Baier, Yu. Dokshitzer, S. Peigné and D. Schiff, Phys. Lett. B**345**, 277–286 (1995).
- [2] R. Baier *QCD, Proc. IV Workshop-1998 (Paris)* Eds, H. M. Fried, B. Müller (World Scientific, Singapore, 1999) pp 272–279.
- [3] M. J. Tannenbaum *ibid.*, pp 280–285, pp 312–319.
- [4] e.g. see *Proc. Int'l Wks. Quark Gluon Plasma Signatures (Strasbourg)* Eds. V. Bernard, *et al.*, (Editions Frontieres, Gif-sur-Yvette, France, 1999).
- [5] M. J. Tannenbaum, Nucl. Phys. A**749**, 219c–228c (2005).
- [6] See Ref. [7] for a more thorough treatment with a full list of references.
- [7] M. J. Tannenbaum, PoS(CFRNC2006)001.
- [8] R. P. Feynman, R. D. Field and G. C. Fox, Nucl. Phys. B**128**, 1–65 (1977).
- [9] S. S. Adler, *et al.* PHENIX Collaboration, Phys. Rev. D**74**, 072002 (2006).
- [10] A. Adare, *et al.* PHENIX Collaboration, Phys. Rev. D**82**, 072001 (2010).
- [11] A. Adare, *et al.* PHENIX Collaboration, Phys. Rev. Lett. **104**, 252301 (2010).
- [12] A. Adare, *et al.* PHENIX Collaboration, Phys. Rev. Lett. **101**, 232301 (2008).
- [13] A. Adare, *et al.* PHENIX Collaboration, Phys. Rev. C**77**, 011901(R) (2008).
- [14] A. Adare, *et al.* PHENIX Collaboration, arXiv:1105.3928v1, submitted to Phys. Rev. Lett.
- [15] G. Aad, *et al.* (ATLAS Collaboration), Phys. Rev. Lett. **105**, 252303 (2010).
- [16] The CMS Collaboration, arXiv:1102.1957v2, submitted to Phys. Rev. C.